Electronic Supplementary Material (ESI) for Lab on a Chip

Supporting Information

Fast, active droplet interaction: coalescence and reactive mixing controlled by electrowetting on a superhydrophobic surface

Angelo Accardo[†,§], Federico Mecarini[†], Marco Leoncini[†], Fernando Brandi[†], Emanuela Di Cola[§], Manfred Burghammer[§], Christian Riekel[§] and Enzo Di Fabrizio[†]

[†] *Istituto Italiano di Tecnologia, Department of Nanostructures, Via Morego, Genova 16163, Italy*

[§] *European Synchrotron Radiation Facility, B.P. 220, F-38043 Grenoble Cedex, France*

ELECTROWETTING-ON-DIELECTRICS (EWOD) PRINCIPLE

An electrowetting device is based on the actuation of an electric field which modifies the wetting behaviour of a polarisable/conductive droplet in contact with an insulated electrode. The law which governs such kind of phenomenon is the Lippmann-Young equation: $\cos\theta = \cos\theta_0 + \frac{1}{2}\frac{C}{\gamma_{LG}}V^2$ where θ, θ_0, C, γ_{lg}, V are respectively the contact angle after applying the electric voltage V, the contact angle without applying any voltage, the capacitance (per surface unit) of the media between the electrodes and the liquid, the surface tension between the drop and the surrounding fluid (air) and the applied electrical voltage. Indeed an electric voltage actuation provokes a decrease of the local contact angle.

In the specific case we calculated a capacitance (per unit surface) of 0.023 mF/m^2. From previous works[1] it is possible to write the expression of the Lippmann Force as $F = \frac{eC}{2}V^2$, where e is the transverse dimension of the electrode (see Fig. 1 taken from [1]).

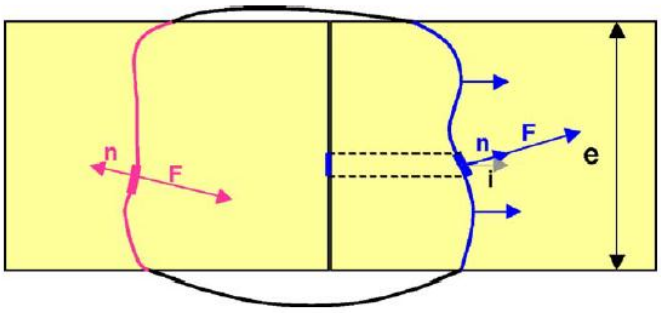

Figure 1. Sketch of the contact of a drop with the substrate[1] (the complete analysis is in [1]).

Using the Lippmann-Young relation[1] , it is possible as well to extrapolate a criterion for droplet displacement which is $\frac{eC}{2}V^2 > e\gamma\alpha\left[\cos\theta+\sin\theta-\cos\theta_0+\sin\theta_0\right]$, where γ is the surface tension between the drop and the surrounding fluid and α is the contact angle hysteresis.

MATERIALS

Na_2CO_3*$10H_2O$ and $CaCl_2$*$2H_2O$ were dissolved in deionized water with concentrations of 100 mg/ml. The PMMA nanocolloidal solution was provided by T. Narayan (ESRF-ID02) beamline.

MICROFABRICATION PROCESSES

The SHEWOD device developed by us requires two separate phases of microfabrication. A 50 μm polyimide stencil mask -developed by laser ablation techniques allows avoiding an optical lithography step, thus speeding-up the microfabrication process considerably. The geometry of the 4 mm^2 interdigited electrodes with a 100 μm inter-gap avoids physical obstruction around the droplets. The polyimide stencil mask was produced by the use of an OPTEC MicroMaster workstation, excimer laser 248nm COMPexPro 110-F (Figure 2C). The stencil mask was used to deposit directly by Physical Vapor Deposition (P=$5x10^{-6}$ mbar) the

metal electrodes, the electrical connections and the pads (Au 300 nm thickness) with a first seed layer of Ti (20 nm). Finally the whole chip (except the external connection pads) has been insulated with a SiO_2 dielectric layer (200nm) by Plasma Enhanced Chemical Vapor Deposition (PECVD) (300°C, 1400 W, 800 mT). (Figure 2B)

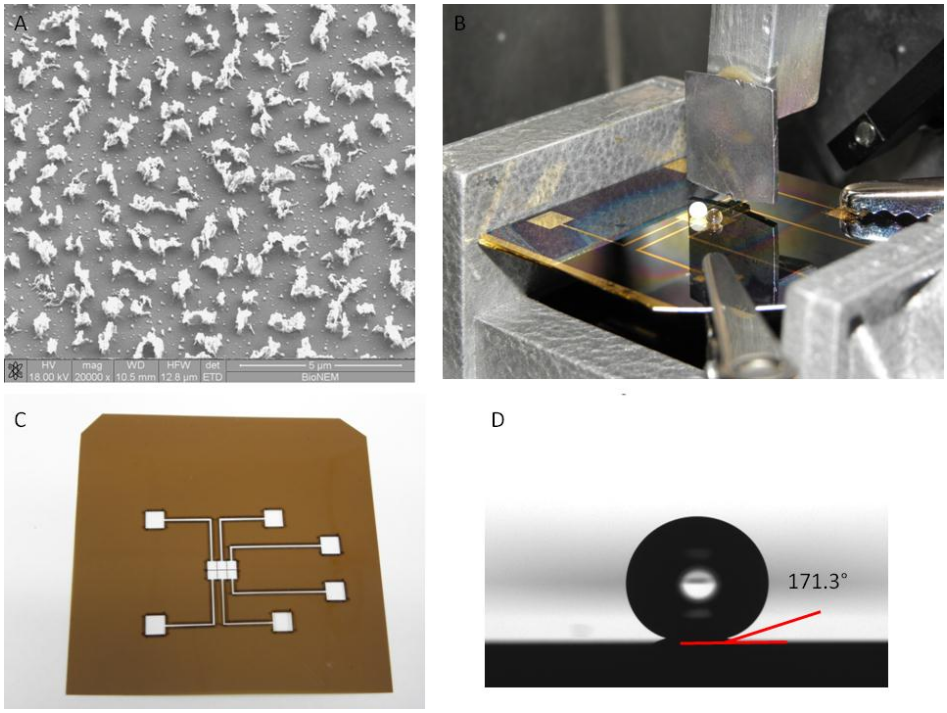

Figure 2. A: SEM image of the PMMA nanostructured layer; B: SHEWOD device integrated into the ESRF-ID13 beamline raster-scanning goniometer. A pierced lead-foil is used for background reduction. A water and a PMMA nanocolloidal solution droplet are deposited prior to mixing. C: polyimide stencil mask; D: Contact angle of a water droplet above the PMMA nanostructured surface.

With respect to the fabrication of the superhydrophobic PMMA layer, we used a liquid PMMA (A11 from MicroChem) and optimized a recipe comprising spinning step (spinning 4K RPM for 60 sec), baking step (30 min at 180°C) and oxygen plasma process (100w, 50w, 33% L, 75% T, 30sccm O_2, 90%tol, P=50mT). Finally the chip was coated by a layer of Teflon using a further plasma process (600 W coil, 0 W platen, 85 sccm C_4F_8, P=27 mT, T=10 s). (Figure 2A) The superhydrophobic properties[2] are confirmed by a contact angle of water droplets of 171.3°. (Figure 2D) Droplets were by a syringe on the SHEWOD device. All experiments were performed in air at about 23°C. A high speed pco.dimax CMOS camera

was used for recording sequences with 5000 frames/s. The video sequence included in the Additional Information corresponds to 1498 frames.

SYNCHROTRON RADIATION EXPERIMENTS and ANALYSIS

The experiments were performed at the ESRF-ID13 beamline.[3] A monochromatic beam of λ= 0.0995081 nm wavelength was focused to a 1.5 (h) * 1.3 (v) μm^2 spot with about 10^9 ph/s flux at the sample position by crossed mirrors. The SHEWOD chip was installed on the ID13 beamline raster-scanning goniometer.[3] (Figure 1B)

A MAXIPIX photon-counting detector based on a 2x2 array of MEDIPIX-2 chips[4] corresponding to 512*512 pixels of 50x50 μm^2 pixel size and a Frelon CCD camera[5] with 2048*2048 pixels of 50x50 μm^2 pixel size were used for data collection. We define as framing time, the time for the collection of a pattern plus the average readout time. For the MAXIPIX detector and 100 ms patterns we determined for a sequence of 1000 frames a framing time of 109 ms while for the 8*8 binned Frelon CCD camera and 100 ms patterns we determined a framing time of 338 ms. The CCD binning allowed optimizing the readout speed but reduced the resolution at low Q-values. We used therefore the MAXIPIX detector for exploring the SAXS-range at the highest data collection speed at the onset of mixing and the Frelon CCD camera for the WAXS-range.

Diffraction experiments were performed at room temperature in air with a typical exposure time of 100 ms/pattern. The distance sample-to-detector was calibrated by Ag-behenate diffraction patterns[6] to 84.2 mm for the SAXS experiments using the MAXIPIX detector and to 205.1 mm for the WAXS experiments using the Frelon CCD camera.

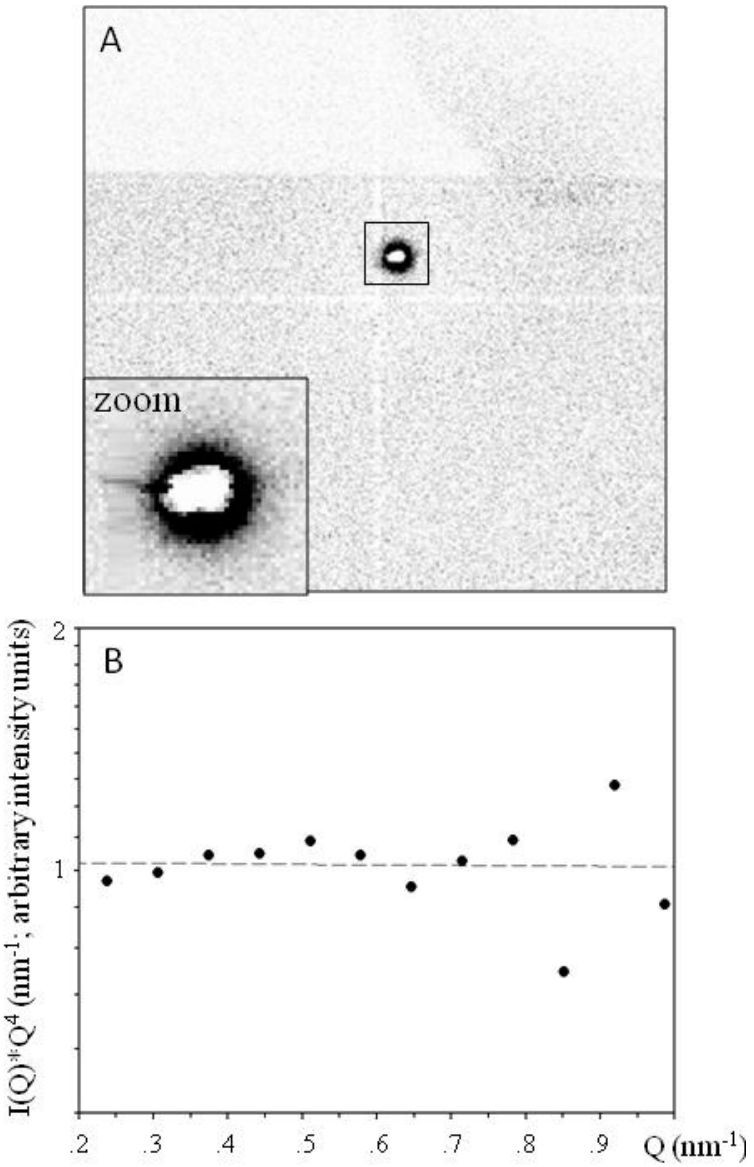

Figure 3 A: SAXS pattern of amorphous calcium carbonate particles recorded with MAXIPIX detector. The cross-like pattern is due to the separation between the 4 MEDIPIX-2 chips. The zoom shows the area which was integrated for the SAXS time-series. B: Porod plot of SAXS pattern at 0.545 sec after onset of mixing (see Figure 3A of article).

The lower Q-limit ($Q=4\pi\sin\Theta\lambda^{-1}$ where Θ is the Bragg angle) of the SAXS experiments is defined by the cut-off of the beamstop at Q_{min}~0.2 nm^{-1}. The upper Q-limit is limited by the dimensions of the MAXIPIX detector to Q_{max}~8.2 nm^{-1}. (Figure 3A) For the Frelon CCD camera, the upper Q-limit is Q_{max}~27.5 nm^{-1}. Only the upper part of the WAXS patterns was analyzed as the lower is shadowed by the substrate. (see Figures 3E,F of article) The SAXS resolution is sufficient to observe the form factor oscillations of nanocolloidal PMMA

solution (see Figure 3A of article). The lack in oscillations of nanocolloidal calcium carbonate is attribute to the decay of the oscillations in the Q-range accessible to the present SAXS-setup.[7] We observe, however, Porod-type behaviour for the SAXS patterns recorded at the onset of the mixing process as expected from three-dimensional particles with sharp interfaces. (Figure 3B) The SAXS-time series were analyzed by integrating the intensity in an area around the beamstop up to Q~0.9 nm^{-1}. (Rectangle in Figure 2A and zoom) The background scattering measured before merging of the droplets was subtracted from all patterns in the series. The WAXS data of the crystalline calcium carbonate modifications were analyzed as described elsewhere.[8]

References

[1] J. Berthier et al., *Sensors and Actuators, A: Physical* **2007**, 134, 2, 471‑479

[2] A. Accardo, F. Gentile, F. Mecarini, F. D. Angelis, M. Burghammer, E. DiFabrizio, C. Riekel, *Microelectronic Engineering* **2011**, *88*, 1660-1663

[3] C. Riekel, M. Burghammer, R. Davies, R. Gebhardt, D. Popov, in *Applications of Synchrotron Light to Scattering and Diffraction in Materials, Vol. 776* (Eds.: T. A. Ezquerra, M. Garcia-Gutierrez, A. Nogales, M. Gomez), Springer, Heidelberg, **2009**, pp. 91-104.

[4] C. Ponchut, J. M. Rigal, J. Clement, E. Papillon, A. Homs, S. Petitdemange, *JINST* **2011**, *6*, CO1069.

[5] J. C. Labiche, O. Mathon, S. Pascarelli, M. A. Newton, G. G. Ferre, C. Curfs, G. Vaughan, A. Homs, *Rev. Scient. Instrum.* **2007**, *78*, 091301.

[6] T. N. Blanton, T. C. Huang, H. Toraya, C. R. Hubbard, S. B. Robie, D. Louer, H. E. Goebel, G. Will, R. Gilles, T. Raftery, *Power Diffraction* **1995**, *10*, 91-95.

[7] J. Bolze, B. Peng, N. Dingenouts, P. Panine, T. Narayan, *Langmuir* **2002**, *18*, 8364-8369.

[8] A. Accardo, M. Burghammer, E. Di Cola, M. Reynolds, E. Di Fabrizio, C. Riekel, *Langmuir* **2011**, *27*, 8216-8222.